Colloid Polym Sci
DOI 10.1007/s00396-017-4149-y

ORIGINAL CONTRIBUTION

Radical polymerization of capillary bridges between micron-sized particles in liquid bulk phase as a low-temperature route to produce porous solid materials

Katharina Hauf[1] · **Kamran Riazi**[2] · **Norbert Willenbacher**[1] · **Erin Koos**[1,3]

Received: 8 May 2017 / Revised: 28 June 2017 / Accepted: 30 June 2017

Abstract We present a generic and versatile low-temperature route to produce macroporous bodies with porosity and pore size distribution that are adjustable in a wide range. Capillary suspensions, where the minor fluid is a monomer, are used as precursors. The monomer is preferentially located between the particles, creating capillary bridges, resulting in a strong, percolating network. Thermally induced polymerization of these bridges at temperatures below 100 °C for less than 5 h and subsequent removal of the bulk fluid yields macroscopic, self-supporting solid bodies with high porosity. This process is demonstrated using methyl methacrylate and hydroxyethylmethacrlyate with glass particles as a model system. The produced poly(methyl methacrylate) (PMMA) had a molecular weight of about 500,000 g/mol and dispersity about three. Application specific porous bodies, including PMMA particles connected by PMMA bridges, micron-sized capsules containing phase change material with high inner surface, and porous graphite membranes with high electrical conductivity, are also shown.

Keywords Membranes · Microparticles · Microscopy (electron, fluorescence) · Phase-change materials · Rheological properties · ^{1}H-NMR · Capillary bridges · Capillary suspensions · Poly(methyl methacrylate) · Radical polymerization

Introduction

Solid porous media are found in a wide range of applications such as in building materials, e.g., porous cement and concrete that are lighter and allow airflow [1], as well as porous pills [2] and pellets with a high surface area [3, 4]. Controlled porosity is also very important in separation devices such as filters, membranes, and microsieves. Depending on the requirements for the separation process, such as micro-, ultra-, nanofiltration, pervaporation, reverse osmosis or gas separation, there is a huge variety of membrane types made from different materials [5].

Producing highly porous media can be realized utilizing different techniques depending on the materials. Glass and other inorganic materials can be directly sintered using particle network formation [6, 7] or solution casting [8]. While sintering is also employed in thermoplastics, like ultrahigh-molecular-weight-polyethylene (UHMWPE) and polytetrafluoroethylene (PTFE) for polymeric membranes [9], other methods can also be used such as stretched films [10–12], nucleation track [13], phase inversion [5, 9, 13–15], extrusion [16], interfacial [17–19], and plasma polymerization [15, 20] or emulsion-templated porous polymers [21]. Each method can produce a range of pore sizes and porosities. Stretching produces bodies with porosities of 90% and very small pore sizes of 0.11 μm [10]. Thermal sintering can yield bodies with pore sizes up to 25 μm and a porosity of 77% [22].

Electronic supplementary material The online version of this article (doi:10.1007/s00396-017-4149-y) contains supplementary material, which is available to authorized users.

✉ Katharina Hauf
katharina.hauf@kit.edu

[1] KIT—Campus Süd, Arbeitsgruppe Angewandte Mechanik, Institut für Mechanische Verfahrenstechnik und Mechanik, Gotthard-Franz-Straße 3, 76131 Karlsruhe, Germany

[2] Institute for Chemical Technology and Polymer Chemistry (ITCP), Karlsruhe Institute of Technology (KIT), MZE, Geb. 30.48, Raum 217, Am Forum 7, 76131 Karlsruhe, Germany

[3] Department of Chemical Engineering (CIT), KU Leuven, Celestijnenlaan 200f, Box 2424, 3001 Leuven, Belgium

Published online: 18 July 2017

Unfortunately, these methods can only be employed for a limited range of materials, e.g., PTFE for filter media, may require a high temperature, e.g., sintering, or require large amounts of organic solvent, e.g., phase inversion. Nearly every method also needs numerous processing steps and may be time consuming.

An alternative way to produce porous polymeric media is to use foams and emulsions stabilized by colloidal particles [23] or particles as sacrificial templates. This method can produce membranes with a very high porosity and narrow pore size distributions of approximately 310 nm [24]. In the work of Feng and Goedel [24], a method is presented where silica particles are used to create porous materials by dissolving the particles with hydrofluoric acid to keep only the polymeric scaffold [24]. A major disadvantage of this method, and sacrificial templates in general, is the additional step to remove the particles, which is done here using an acid that has a significant health risk and may not be completely removed from the membrane. Additionally, a porous and hybrid material made with reactive particles cannot be manufactured with this method. A processing time of almost 2 days is also a disadvantage of this method and has to be adapted to an industrial scale.

There have been other investigations using particles as a wall material to produce porous membranes, for example, with wet granular media as a precursor. Hemmerle et al. [25] used this method for local agglutination of micron-sized particles where glass beads (diameter 55 to 2040 μm) were mixed with polydimethylsiloxane (PDMS) and a curing agent in a mortar with a pestle and afterwards compressed into a desired shape. To crosslink the PDMS between the particles, samples were heated for 14 h at 75 °C. While Hemmerle et al. showed very nicely how the bulk material properties could be varied by changing the number and size of particles and bridging material, they were only able to produce samples with a narrow range of porosities between 41 and 47%.

Another example was presented by Kiesow et al., where bicontinuous composite membranes were made out of a zeolite monolayer and diurethane dimethacrylate (HEMATMDI) as monomer [26]. Capillary forces between the zeolite particles at the air–monomer–water interface kept the particles together. However, the porosity in this system only results from the porous structure of zeolite with pore sizes 4 to 5 Å. This method does not offer a clear way to control the pore size, porosity, or associated physical properties. Furthermore, the porous layer of these membranes can be only a single particle layer thick.

We present a new method using capillary suspensions as a precursor for porous media with a defined porosity and pore size that can be manufactured at a temperature below 100 °C with less time and effort than existing methods. Capillary suspensions are formed by adding a small amount of a secondary fluid that is immiscible with the bulk fluid phase to a particle suspension [27]. The rheological properties can be tuned in a wide range, e.g., the yield stress can be increased by several decades as the mixture transforms from fluid-like to gel-like behavior or from a weak to a strong gel. The change in the strength of these capillary suspensions arises due to the capillary forces between micron-sized particles, which lead to the formation of a percolating particle network. This network and the bridges between the particles have previously been directly visualized with a confocal microscope [28]. There are two extrema for the shape of the capillary bridges between the particles in the suspension depending on the three-phase contact angle $\theta_{S,B} > 90°$, which the secondary fluid S makes against the solid when surrounded by the bulk fluid B. If the secondary fluid preferentially wets the particles ($\theta_{S,B} < 90°$), the system is arranged in the pendular state and the particles are directly connected by capillary bridges, which lead to a sample-spanning network. In contrast, the system is in the capillary state with contact angles $\theta_{S,B} > 90°$, where particle clusters are formed. The particle networks in the pendular state tend to be stronger than in the capillary state with the same solid–liquid–liquid system [28, 29]. This method has already been used to produce porous materials where either the particles are sintered or a reactive epoxy resin is used as the secondary fluid, finally resulting in a solid porous body [22]. In this latter case, a porous (60–75% porosity), lightweight, and conductive graphite-based material with a narrow pore size distribution (d_{50} = 15 μm) was produced. A similar method was shown by Domenech et al. using a ternary mixture of polyisobutylene, polyethylene oxide and silica particles [30]. A drawback of using epoxy or PEO is that of the limited options regarding control of mechanical and other physical or chemical properties.

This paper presents an optimized way to solidify capillary bridges between micron-sized particles in a liquid bulk using a monomer as the bridging fluid. The capillary suspension is then heated under defined conditions to polymerize the bridges. A porous body, with porosity >50%, remains after the bulk fluid is removed. The resulting network consists of particles that are interconnected by polymeric bridges and has been demonstrated here for several fluid combinations. The characteristic dimension of these bridges is on the order of microns, i.e., approximately 100 times larger than the radius of gyration Rg of the produced polymer molecule. Therefore, the polymer is not confined and the resulting polymer is equivalent to bulk polymerization [31, 32]. However, as in suspension polymerization, the heat transfer should be different from bulk polymerization. In this paper, a proof of concept was made using glass spheres as solid phase. This enabled an easy extraction of polymeric bridges needed for further analysis. A general chemical characterization of the polymeric bridges, made from poly(methyl methacrylate) (PMMA) with benzoyl peroxide (BPO) as initiator at temperatures below 100 °C and polymerization times below 5 h, was completed. Chemical composition and molecular weight distributions of the polymeric bridges as well as reference PMMA samples are

compared and discussed. Finally, simplified application-specific bodies using different particles and monomers are shown.

Experimental section

Materials

Hollow glass spheres (iM16K and iM16K OTES) were provided by 3M Deutschland GmbH (Neuss, Germany) with a diameter $d_{50} = 20$ μm and a density of 0.46 g/cm^3. They had a hydrophilic (iM16K) or hydrophobic (iM16K OTES) surface (see Figs. S1 and S2 in the Supplementary information). The monomers were methyl methacrylate (MMA) (≥99%, Carl Roth) with a density of 0.94 g/cm^3 and hydroxyethylmethacrylate (HEMA) (≥99%, Sigma-Aldrich) with a density of 1.07 g/cm^3. Both monomers were used as secondary phases. The initiator for both monomers was benzoyl peroxide (BPO) (75% water remaining Luperox A75, Sigma-Aldrich). Distilled water and paraffin oil (low viscosity, Carl Roth) were used as bulk fluids. All items were used as received. For the application routes, we used the following: (a) poly(methyl methacrylate) particles (Altuglas BS 130) from Altuglas International (Arkema Group, La Garenne-Colombes, France) with a $d_{50} = 20$ μm and a density of 1.19 g/cm^3; (b) phase change material capsules (Micronal DS 5038 X), consisting of a PMMA shell and a core filled with paraffin wax, provided by BASF SE (Ludgwigshafen, Germany) with $d_{50} = 5.2$ μm particles and a density of 0.98 g/cm^3; and (c) graphite particles provided by China Steel Corporation (Kaohsiung, China) with a primary particle diameter $d_{50} = 7.8$ μm and a density of 2.27 g/cm^3.

Sample preparation

The solid–liquid–liquid combinations we used are shown in Table 1.

To prepare the capillary suspensions, the particles were dispersed in the bulk fluid with a high-shear dissolver stirrer (35 mm diameter for confocal microscopy and 60 mm diameter for the polymerized samples) at 1200 rpm for 10 min with a solid volume fraction $\Phi_{\text{glass spheres}} = 40$ vol%, $\Phi_{\text{PMMA}} = 25$ vol%, $\Phi_{\text{Micronal}} = 35$ vol%, and $\Phi_{\text{Graphite}} = 20$ vol%. The monomer and initiator were premixed with a magnetic stirrer at 500 rpm for 5 min where the concentration of initiator in monomer was varied between 5, 10, and 15 mg/ml. This secondary liquid phase was added to the suspension and mixed first at 2000 rpm for 2 min. Then, the speed was decreased to 800 rpm for 5 min of additional mixing. The amount of secondary fluid was 0, 1, 2, 4, or 6% (12% for graphite/HEMA) by volume (Φ_{sec}). This procedure and the subsequent polymerization are shown in Fig. 1.

Polymerization procedure

The prepared capillary suspensions were filled in silicone baking molds (35 mm diameter, 5 mm height). They were then polymerized in the mold, which was placed inside a preheated desiccator set in a laboratory oven. The samples were placed in the desiccator at a starting temperature close to the desired polymerization temperature. The temperature was confirmed with a thermometer inside the oven. Polymerization was done at temperatures of 60, 85, and 120 °C, and polymerization times of 1.5, 2.5, 3.5, and 5 h were employed.

The solid samples with MMA as secondary phase were cooled overnight at room temperature under the hood to interrupt the polymerization and dried afterwards at 74 °C in an oven for 4 h. Any residual BPO and MMA are expected to be unaffected by this drying step due to the low diffusion within the solidified sample. Samples with HEMA were cooled overnight at room temperature and placed on a paper towel for 1 day to remove most of the paraffin oil. Then, the remaining paraffin oil was extracted for 4 h with *n*-hexane (VWR Chemicals). For each sample, references were prepared using the same amount of monomer and initiator in an open glass vial, which was added to the oven with the other samples for polymerization under identical polymerization conditions.

Characterization

Yield stress measurements were performed with the stress-controlled rheometer Haake RS 150 (Thermo Scientific, Karlsruhe, Germany) using a vane geometry (10 mm diameter, 1 mm gap height) by increasing the shear stress stepwise in a range from 0.1 to 1000 Pa. The temperature for all measurements was $T = 20 \pm 0.5$ °C. The yield stress was defined using the tangential method [7].

The capillary bridges between the glass spheres in the wet state prior to polymerization were imaged using a confocal microscope (TCS SP8, Leica Microsystems) with a 552-nm laser. These samples were prepared without the initiator and a fluorescence dye was added to the monomer. Nile red (Sigma-Aldrich, Steinheim, Germany) was used for MMA samples and rhodamine B (Sigma-Aldrich, Steinheim, Germany) for the HEMA system. Glycerin was added in a ratio of 61/39 wt % (glycerin/water) to adapt the refractive index of MMA and water.

The samples were also inspected after polymerization using an environmental scanning electron microscope (ESEM-mode at p = 70 Pa, Quanta 650 FEG, FEI, Hillsboro, Oregon, USA) and images were taken from a fractured section of the solid samples. The samples were sputtered with a mixture of platinum and palladium.

Table 1 Composition of capillary suspensions used in this paper

Solid phase	Bulk fluid	Secondary fluid	Initiator
Hydrophobic glass (iM16K OTES)	Dist. water	MMA	BPO
Hydrophilic glass (iM16K)	Paraffin oil	HEMA	BPO
PMMA (Altuglas BS130)	Dist. water	MMA	BPO
Paraffin wax, acrylate shell (Micronal DS)	Dist. water	MMA	BPO
Graphite	Paraffin oil	HEMA	BPO

Energy-dispersive X-ray spectroscopy (EDX) was also carried out on the fractured samples. Microtomography was performed at Freudenberg SE (Weinheim, Germany) with a computer tomography device (General Electric, Phoenix X-Ray VTOME|X 240 D) using a 240-kV direct X-ray.

The samples made with PMMA as polymeric bridges and the corresponding reference samples were characterized to determine the effect of varying polymerization conditions using size exclusion chromatography (SEC) and nuclear magnetic resonance spectroscopy (^{1}H-NMR). The samples were prepared by dissolving the solid porous material in tetrahydrofuran (THF, Sigma-Aldrich) in an ultrasonic bath for 1 h. The medium was filtered (1.6 μm pore size, Por. 4/5) to separate the glass spheres, and then the THF was evaporated in a rotation evaporator (Büchi) at 55 °C and 385 mbar. Afterwards, the remaining polymer was dried overnight in a laboratory oven at 70 °C and then redissolved in a solvent at a specific concentration depending on the following measurement.

The molecular weight distribution of the polymeric bridges and reference polymers were measured using size exclusion chromatography (SEC), which was operated with THF (Scharlan, SEC-grade) as solvent and calibrated with linear PMMA standards. The instrument consists of an Agilent 1100 pump, and the sample separation was achieved via two linear columns provided by PSS (SDV-Lux −10^3 Å and 10^5 Å and 5 μm). It was equipped with an Agilent 1200 differential refractive index (DRI) detector. Measurements were performed at 25 °C with a flow rate of 1 ml/min. The polymer concentration was approximately 2 mg/ml, and the injection volume was 100 μl. The functional groups were determined with ^{1}H-NMR (400 MHz, $CDCl_3$) carried out using a Brucker Avance III Microbay 400 MHz (typically 1024 scans). Chloroform (Deutero, 99.8%) was used as a solvent at a polymer concentration of approximately 15 mg/ml.

The porosity ε of the solid bodies was calculated using the ratio of the raw density of the sample and the skeletal density.

$$\varepsilon = 1 - \frac{\rho_{\text{raw}}}{\rho_{skeletal}} \quad (1)$$

The raw density of the sample was calculated as the ratio of sample weight and volume. The skeletal density was measured using a multivolume gas pycnometer (Model MP 1305 with Helium) at 20 °C. The flexural strength characterizing the mechanical strength of the solid porous materials was measured using a 4-point bending test on a custom-made device following DIN EN 843-1.

Results and discussion

Rheological behavior

The prepared suspensions showed a nearly two decade increase in yield stress with increasing secondary phase content as shown in Fig. 2. This increase indicates the creation of a sample-spanning network caused by the strong attractive capillary forces between particles. The high yield stress implies the existence of a percolated particulate network, which should be strong enough to resist destruction during molding and polymerization so that a body with high open porosity can be formed. Furthermore, the high yield stress implies the

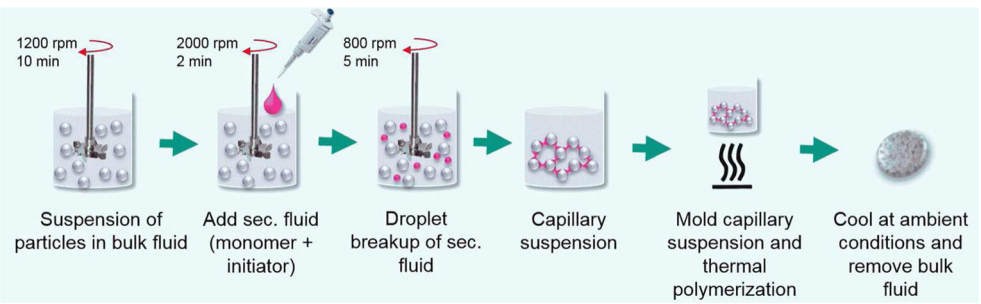

Fig. 1 Processing route for preparation of capillary suspensions and solid porous materials

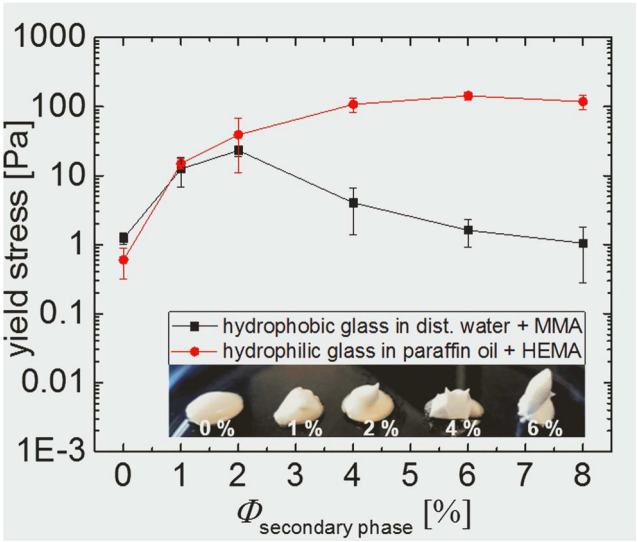

Fig. 2 Yield stress of capillary suspensions made from hydrophobic glass spheres (φ_{solid} = 40 vol%) in distilled water with MMA as secondary phase (*black squares*) and hydrophilic glass spheres (φ_{solid} = 40 vol%) in paraffin oil with added HEMA (*red circles*). The *inset images* show the constistency of the HEMA sample. *Lines* are to guide the eye

presence of a network backbone, which can transmit forces so that the final porous body should also have a high Young's modulus [33].

The sample with hydrophilic glass spheres shows a continuously increasing yield stress with increasing amount of added HEMA. The sample with added MMA, however, has a maximum yield stress at Φ_{sec} = 2 vol%. The existence of such a maximum can indicate the transition from the pendular to the funicular state as larger agglomerates are formed with increasing amounts of secondary liquid [28, 34]. This transition typically occurs at $\Phi_{sec}/\Phi_{solid} \approx 0.1$–0.2 depending on the contact angle and coordination number [6, 28, 35, 36]. Our results for the glass/MMA system are consistent with these earlier findings. The capillary suspensions made from hydrophilic glass spheres with paraffin oil as the bulk liquid and HEMA as secondary fluid were stable and homogeneous for more than 5 days. This stability is typical for a capillary suspension. However, phase separation was observed after 10 min for the system with hydrophobic glass spheres, water as bulk fluid, and MMA as secondary fluid phase. For this MMA sample, the particles with the dyed MMA showed creaming behavior.

Visualization before and after polymerization

To confirm if the increasing yield stress was caused by the capillary force and to determine if such agglomeration might occur, the microscopic configuration was imaged to visualize the existence of capillary bridges and their shape between the particles. A capillary suspension with MMA as secondary fluid in the wet, unpolymerized state as obtained from confocal microscopy is shown in Fig. 3.

This sample used a water/glycerine mixture as a bulk fluid to match the refractive indices and 6 vol% dyed MMA as the secondary phase. The sample with 2% MMA was not visible because of the low fraction of secondary phase reducing the overall amount of fluorescent dye. The particles in this image are visible as dark circles because of their hollow character. The MMA (red) is located in between the particles and creates bridges. Most of these bridges appear to join more than two particles, forming a funicular network. While there may be a large number of binary interactions, which can be more difficult to image due to their smaller volume, a small number of these funicular clusters can monopolize a large fraction of the available secondary fluid [28]. The general shape of the specimen can be preserved during the polymerization process as is presented in Fig. 4a. Particle distribution within the polymerized samples and shape of individual capillary bridges is shown in Fig. 4b.

In the samples shown in Fig. 4, the BPO content was 15 mg/ml MMA and the polymerization time and temperature were 82 °C for 2.5 h. The particles are connected by the polymerized PMMA bridges, which are still located between the particles and still possess a pendular shape. Remarkably, these bridges are not a uniform block of PMMA, but appear to have an irregular texture. This may be due to the shrinkage of the material during the polymerization process. These SEM images also show that the hollow glass spheres have a wide size distribution. This may offer a tunable parameter to control the pore size and porosity of the produced samples [6].

We also tested a second system using hydrophilic glass spheres in paraffin oil with HEMA as the secondary fluid. This system, with dyed HEMA, is shown in Fig. 5.

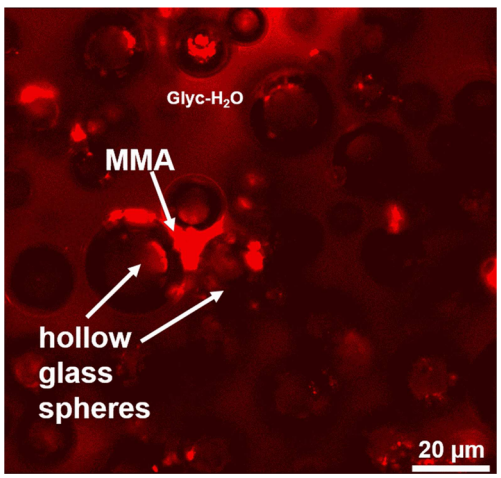

Fig. 3 Confocal image slice for the hydrophobic hollow glass spheres in glycerin/water mixtures (61/39 wt%) with 6 vol% added MMA. The MMA is dyed (*red*), and the other components are undyed

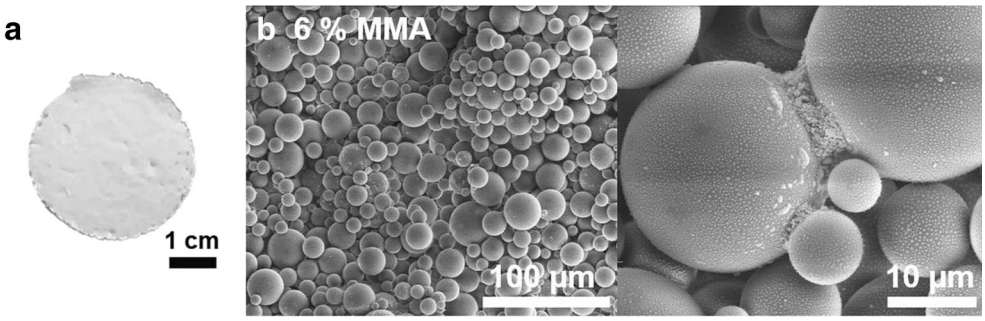

Fig. 4 **a** Image of a porous solid sample made from hydrophobic hollow glass spheres with PMMA bridges with 6 vol% MMA. **b** Corresponding ESEM images of a fractured section of the body and the bridges. The samples were polymerized in water for 2.5 h at 82 °C, and the BPO content was 15 mg/ml.

For this sample, both large clusters (Fig. 5a) and binary pendular bridges (Fig. 5b) are visible. Polymerization also works well, if not better, in this system, as shown in Fig. 6. These two systems demonstrate the versatility of this method where either hydrophilic or hydrophobic particles can be linked together with a judicious choice of the monomer and the bulk fluid. For the HEMA system, the bridges are smooth and clearly defined, though the particles are rough. The atomic composition of both the neck and the particle surface was investigated using EDX in the ESEM mode (Fig. S4). The bridges do not contain any silicon, just carbon and oxygen, suggesting that the bridges are made from polymer. EDX of the particle surface shows a mixture of carbon, oxygen, and silicon.

Note that the porosity of the solid bodies is equal to the fraction of bulk fluid in the samples. In contrast to porous sintering materials made from capillary suspensions, no collapse of the particle network during drying and debinding or shrinkage during sintering does occur here, i.e., porosity is directly determined by particle concentration. However, for the samples with the highest particle loading, a substantial amount of air was entrapped during paste preparation leading to an even higher porosity of the final dry specimen and additional larger pores >50 µm, see µ-CT image in S3 (Supplementary information).

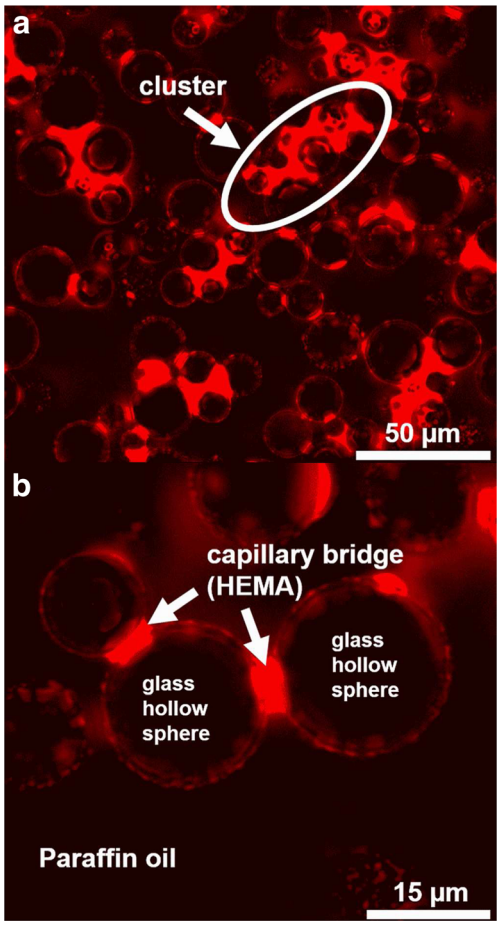

Fig. 5 Confocal image slice for the hydrophilic hollow glass spheres in paraffin oil with 4 vol% added HEMA. The HEMA here is dyed (*red*), and the other components are undyed. The circle shows a cluster of particles connected by the secondary fluid

Chemical composition of polymeric bridges

Chemical composition of polymerized bridges has been analyzed using ^{1}H-NMR spectroscopy. A comparison of the reference sample and material polymerized in the bridges (Fig. 7) shows that their chemical composition is similar and the main expected signals for PMMA are present in each sample.

The peak at 3.60 ppm corresponds to the methyl ester-group found in PMMA [37]. The peaks in the region between $\delta = 2.2$ and 1.3 ppm are significant for the CH_2-group [38]. The peaks at $\delta = 1.2$ and 0.84 ppm correspond to the *cis*- and *trans*-configurations of α-CH_3-group [38], and the sum of their integral intensities should be equal to the intensity of the peak at $\delta = 3.60$ ppm. This was confirmed for each measured spectrum.

The insert in Fig. 7 shows that additional peaks at $\delta = 8.14$ ppm and $\delta = 8.12$ ppm occur for the capillary bridge sample with the lowest initiator concentration of 5 mg BPO/ml MMA. This indicates that not all of the free radicals generated from the BPO initiate polymeric chain growth in this case, but immediate recombination occurs [39]. The pathways for decomposition of the initiator and corresponding polymeric chain growth are explored in the following section.

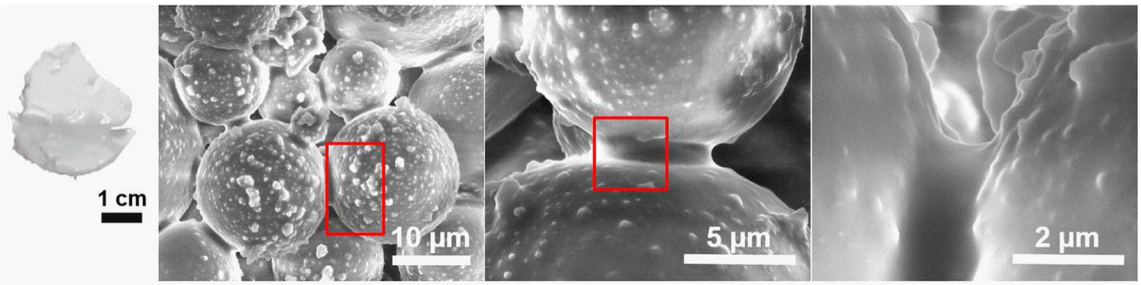

Fig. 6 Image of a piece of porous solid samples made out of 40 vol% hydrophilic hollow glass spheres interconnected with poly(HEMA)-bridges with an amount of 4 vol% HEMA in the wet state (15 mg/ml BPO, polymerization in paraffin oil at 82 °C for 2.5 h), and corresponding ESEM images of a fractured section. The magnification of the ESEM images increase from *left* to *right*

Degree of polymerization in capillary bridges

Conventional bulk polymerization is expected to take place in the monomer bridges between the particles. Since the monomeric bridges in the percolated network of particles have a characteristic size ≈1 µm and are surrounded by a bulk fluid, the anticipated chemical reaction can also be regarded as a type of suspension polymerization. To characterize the molecular weight and dispersity of the polymers synthesized in the bridges, we use the MMA system with hydrophobic glass particles and water as the bulk fluid. BPO was dissolved in MMA to induce a radical polymerization within the capillary monomer bridges. The initiation of polymerization consists of two steps. First, the BPO molecule is decomposed into two radicals, a process that is thermally triggered. Then, the MMA bonds to the initiating radical. This process is shown below. Red arrows with half-heads show where single electrons are shifted.

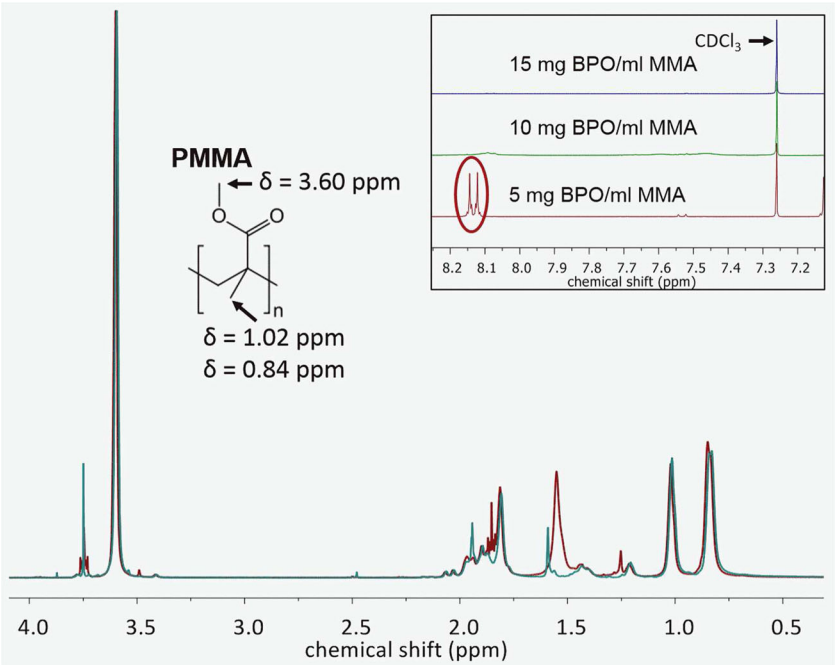

Fig. 7 ^{1}H-NMR with the chemical shift for the relevant functional groups for PMMA in the reference sample (*green*) and the bridges (*red*). Peaks for PMMA at δ = 3.60 ppm, δ = 1.02 ppm, and δ = 0.84 ppm are visible in both samples. The latter two peaks provide information about atactic and syndiotactic arrangements of the PMMA chains. The sum of their integral intensity equals that of the peak at δ = 3.60 ppm. The peaks in the region between δ = 2.2 and 1.3 ppm are significant for the CH_2-group [37]. Differences between the bulk and capillary bridge samples occur in this δ range, which are presumably due to impurities inferred from the preparation of the capillary suspension. *Inset box*: ^{1}H-NMR signals corresponding to initiator BPO and solvent $CDCl_3$ for capillary bridge samples with different initiator concentrations. The samples were prepared with 15 mg/ml BPO for 2.5 h at 87 °C, and the spectra were normalized using the chemical shift at δ = 3.60 ppm.

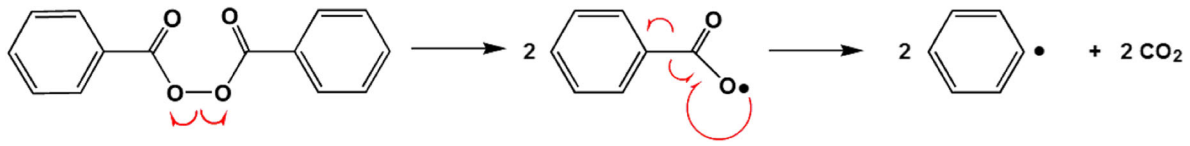

Either of the radicals, benzoyloxy or phenyl (showed in the following scheme as I: initiator), can attach to a monomer unit and start a polymer chain. In the chain propagation phase, additional MMA molecules attach to the MMA radicals until chain termination takes place.

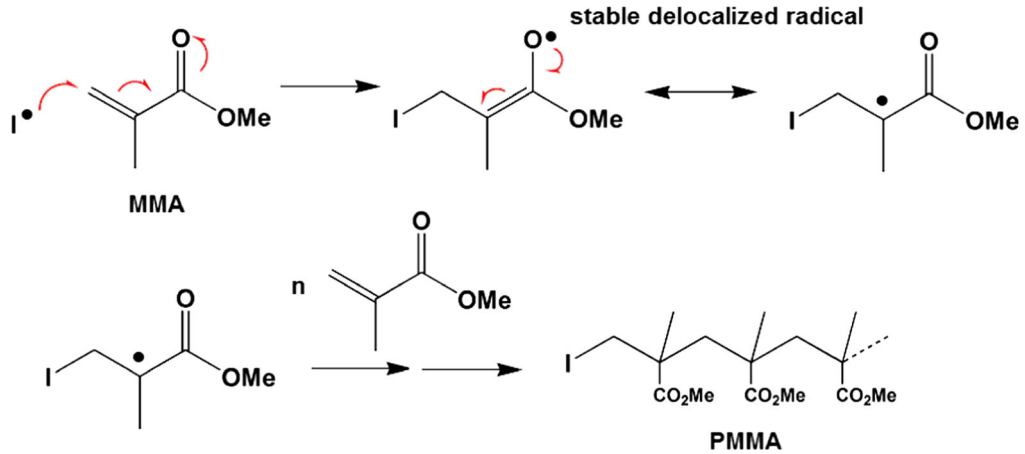

The termination is caused by the self-reaction of propagating radicals through combination and/or by disproportionation, where a free electron from a radical is transferred to another chain radical and a new double bond is created.

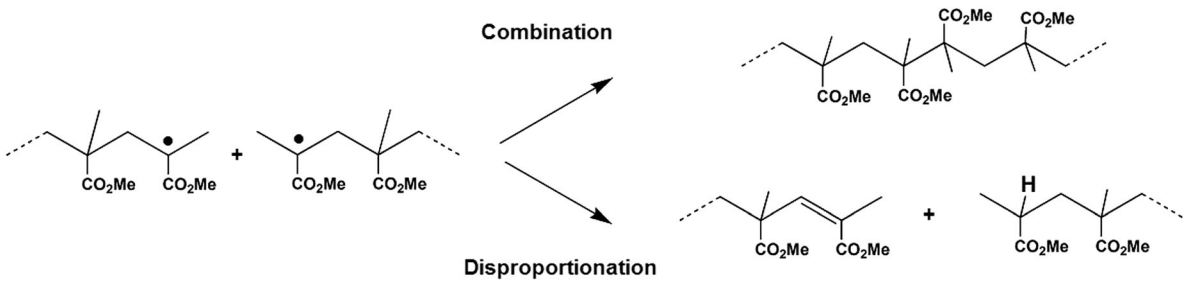

The kinetics of free radical polymerization lead to a polymerization rate k_d depending on the square root of the initiator concentration [40],

$$k_d \propto \sqrt{[I]} \tag{2}$$

where k_d is related to the initiator half-life $t_{1/2} = \ln 2/k_d$ that is defined as the time needed to reduce the concentration of the initiator by half. The half-life for BPO depends on temperature and has a value of 7.3 h at 70 °C, 1.4 h at 85 °C, and 20 min at 100 °C [40].

The number average degree of polymerization P_n of the macromolecules produced via free radical polymerization is proportional to the reciprocal square root of initiator concentration [41].

$$p_n \propto \frac{1}{\sqrt{[I]}} \tag{3}$$

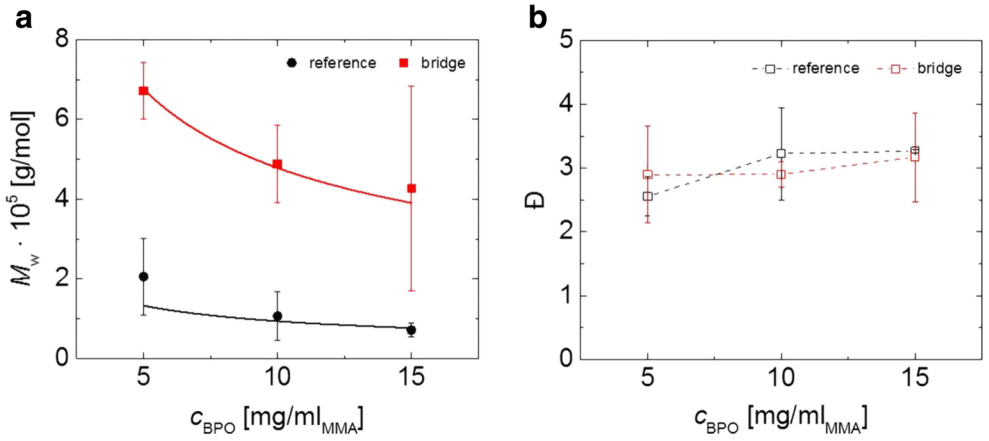

Fig. 8 **a** Dependence of BPO concentration on molecular weight M_w for polymeric bridges and reference PMMA samples. The *solid lines* represent the molecular weights predicted by Eq. (3), with proportionality constants of 15 (bridges) and 3 (reference). **b** Dependence of BPO concentration on dispersity $Đ$ for polymeric bridges and reference PMMA samples. *Lines* are to guide the eye. Both parts show a capillary suspension with 40 vol% hydrophobic glass particles, 6 vol% MMA as secondary fluid and distilled water as the bulk fluid. The polymerization for both the bridges and reference sample occurred at 84 °C for 2.5 h.

Ergo, the molecular weight of the macromolecules obtained by free radical polymerization, should decrease with increasing initiator concentration.

We determined the dependence of BPO concentration on the resulting molecular weight and dispersity for the polymeric bridges and a reference sample using SEC. Both the reference and the bridges are subjected to identical conditions during polymerization. The dispersity $Đ$ is defined as ratio between the weight-averaged molecular mass M_w and the number-averaged molecular mass. As can be seen in Fig. 8, the average molecular weight M_w decreases with increasing BPO concentration caused by the increased number of free radicals that are able to simultaneously react with the MMA monomers. This reduction is consistent with the dependence on the initiator concentration, outlined above, where predictions using Eq. (3) are shown in Fig. 8 as solid lines. An example molecular weight distribution for a bridge sample extracted after polymerization of a capillary suspension with 40 vol% solid fraction and 6 vol% MMA at 84 °C for 5 h with 15 mg/ml BPO, as obtained from SEC, is shown in S4 (Supplementary information). Similar molecular weight distributions were found for all other investigated samples.

As shown in Fig. 8, the mean molecular weight obtained in the polymerized bridges is, on average, 2.8 ± 0.15 times higher than the values for the corresponding reference PMMA samples. This is qualitatively expected for two reasons. First, the heat transfer in the small bridges mediated by the surrounding water phase and hollow glass spheres is lower than in the bulk and the mobility of polymer chains is inhibited due to gelation effects, i.e., the disproportionation is less

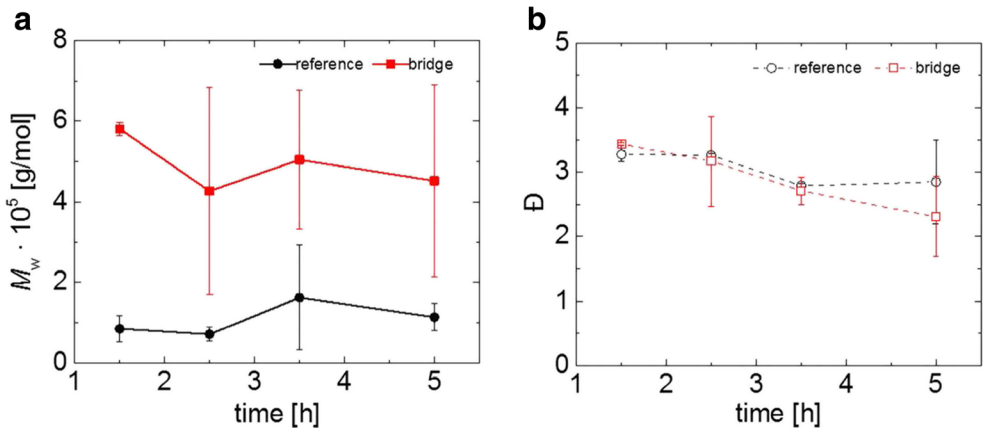

Fig. 9 **a** Dependence of polymerization time on molecular weight M_w for polymeric bridges and reference PMMA sample. **b** Dependence of polymerization time on dispersity $Đ$ on polymerization time for polymeric bridges and reference PMMA sample. *Lines* in **a** and **b** are to guide the eye. The capillary suspensions were made of 40 vol% solid fraction and 6 vol% MMA with distilled water as the bulk fluid. Each measurement was carried out at 84 °C for 2.5 h and with 15 mg/ml BPO.

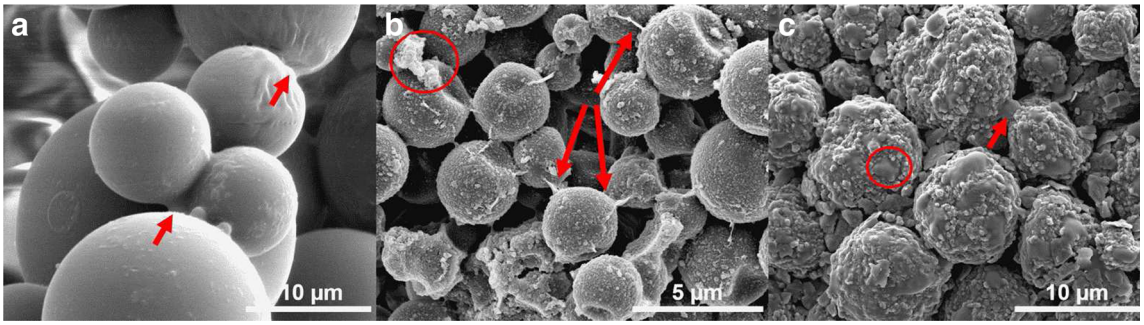

Fig. 10 SEM images of porous solids made from capillary suspensions with polymerized bridges. Different particles and secondary fluids were used. **a** 35 vol% PMMA particles, 3 vol% MMA. **b** 35 vol% Micronal DS particles, 3 vol% MMA. **c** 20 vol% graphite particles, 12 vol% HEMA. Polymerization was always done at 82 °C for 2.5 h with 15 mg/ml BPO as initiator

probable [38]. Second, the high surface-to-volume ratio of the capillary bridges could result in a significant geometrical effect, which causes a mobility barrier for the polymer chains and macroradicals. It was shown in a previous work for suspension polymerization that the molecular weight increases slightly with decreasing polymer particle size [42, 43]. The dispersity remains constant upon initiator variation within experimental uncertainty such that, in both the bridges and reference samples, $Đ = 3 \pm 0.5$ is found.

In another set of experiments, the effect of polymerization time on molecular weight distribution was investigated. The polymerization time has no significant influence on the average molecular weight M_w of the pure sample and the polymeric bridges at a single temperature of 84 °C, but the dispersity seems to decrease slightly, as is shown in Fig. 9. We can, therefore, use a time of 3.5 h, which is more than twice the half-life of the initiator, as a convenient polymerization time since the PMMA has a sufficiently high molecular weight and a dispersity index less than 3. Again, the average molecular weight of the capillary bridges is about three times higher than for the respective bulk samples. Because of the purification and separation steps needed to extract the polymeric material from the capillary suspension, yield measurements were not possible.

Similar results regarding molecular weight distribution were obtained at other polymerization temperatures T in the range of 60 and 120 °C with a slight decrease with increasing T (at given BPO concentration and polymerization time) as expected due to the higher rate of initiator decomposition at higher temperatures [40]. According to the half-life $t_{1/2}$ of 7.3 h at 60 °C very long times >15 h are required to complete polymerization.

With respect to the fabrication of porous solid materials based on capillary suspensions concept, we emphasize that PMMA bridges can be efficiently polymerized at temperatures below 100 °C and the concept can be used even for temperature sensitive particles that might melt or decompose at elevated temperatures.

Application routes

In addition to the model system with glass spheres, where a chemical reaction between the glass surface and the polymeric bridge can be excluded, we also tested other systems with potential technical relevance. These systems both demonstrate the versatility of this method and show how the properties are modified by the material choices. All of these systems are shown in Fig. 10.

The first system, shown in Fig. 10a, is made from a capillary suspension including 35 vol% crosslinked PMMA particles and 3 vol% added MMA including 15 mg BPO/ml MMA as the secondary liquid. The confocal image S6 (Supplementary information) reveals that the dyed MMA completely coats the particles since it spreads extremely well on the PMMA surface. While it is not visible in the confocal image, there remains some MMA that bridges the particles. These bridges are visible in the SEM image (Fig. 10a), where polymerized bridges are located between the particles (as denoted by the arrows) and lead to a self-supporting membrane with flexural strength of 0.008 MPa at a given open porosity of 79%.

We also fabricated porous bodies from micron-sized phase change material (PCM) particles coated with highly crosslinked PMMA. Porous materials made out of small encapsulated PCM particles may be applied as heat exchange materials offering superior heat transfer rates due to the large inner surface. Possible examples include thermally insulating paint or thin thermal interface layers in electrical devices. As shown in Fig. S7, the dyed MMA coats these particles just as it does for the pure PMMA particles. In Fig. 10b, string like structures (red arrows) are the polymeric connections between the particles. The red circled structure is likely due to additives as they are also observed on the samples without any added MMA as secondary phase. The stress at failure was measured to be 0.5 ± 0.1 MPa at an open porosity of 48.4 ± 0.8%, which is in the expected range estimated for porous PMMA based on the Gibson–Ashby model for porous materials and mechanical strength data of pure PMMA [44].

A third system made from graphite particles (Φ_{solid} = 20 vol%) with HEMA (12 vol%) as secondary phase and paraffin oil as bulk fluid is shown in Fig. 10c. The pure graphite particles are shown in Fig. S8. The poly(HEMA) forms the bridges between graphite particles (arrow) and patches on the particles (circle). In this case, the poly(HEMA) is able to preserve a porosity of 60% in the graphite body. More importantly, this body is conductive with a value of 13 mS/cm. The pure powder (ρ_{bulk} = 0.83 g/cm^3) has a conductivity of 30 mS/cm. If we consider the conductivity divided by the graphite mass in the samples, we can get almost the same conductivity per mass of 7.64 mS/(cm g) for the graphite-poly(HEMA)-composite as for pure powder with 8.3 mS/(cm g). This demonstrates that our polymerization strategy enables fabrication of porous hybrid membranes made out of graphite particles and polymeric bridges with high electrical and, presumably, good thermal conductivity.

Conclusions

Capillary suspensions in the pendular and funicular state can be used as a precursor for local adhesion of micron-sized particles. These solid–liquid–liquid systems are created when a small amount of a liquid, immiscible with the bulk, is added to a suspension. This secondary liquid creates capillary bridges between the particles and results in a strong, percolating network. This method offers a novel way to produce porous bodies by preserving the network structure during the transition from liquid capillary bridge, formed here by a monomer, to a solid polymeric bridge. This method can be realized at temperatures below 100 °C for times less than 5 h, i.e., it is non-destructive to various kinds of particles. The material properties of the resulting porous sample can be controlled by choosing the particles and monomers as well as the bulk material.

We used a model system made of glass spheres, monomer with initiator as secondary fluid, and a bulk fluid that is immiscible with the monomer. Hydrophobic and hydrophilic glass particles with methyl methacrylate (MMA) and hydroxyethylmethacrlyate (HEMA), respectively, as capillary bridges were used for this proof of concept. This glass model system allows for a convenient imaging of capillary bridges and separation from the particles for further chemical characterization. The formation of a sample-spanning network was confirmed through yield stress measurements and also through direct imaging using a confocal microscope. The capillary suspensions were polymerized to solidify the capillary bridges and dried to produce solid porous bodies. These were imaged using SEM imaging with EDX analysis of the bridge material and the glass spheres. ^{1}H-NMR confirmed that polymerization took place and the MMA was successfully converted into polymer. The lowest concentration of 5 mg BPO per ml MMA may cause incomplete conversion and residual BPO remains in the final polymer. SEC analysis shows that the average molecular weight in the bridges is 2.8 ± 0.15 times higher than the values for the bulk PMMA reference samples. This difference in molecular weight is attributed to the high heat transfer and the large surface-to-volume ratio of the small monomer fluid volumes surrounded by particles and bulk fluid. The molecular weight scales with the reciprocal square root of the initiator (BPO) concentration. This dependence allows the polymer molecular weight in the particle bridges and the corresponding bulk properties to be controlled. The molecular weight shows no dependence on the polymerization time and only a slight decrease with increasing temperature making this method fairly robust. The dispersity is affected neither by BPO concentration nor by changes to the polymerization time and temperature.

The applicability of the concept to particle systems with potential technical relevance was shown using PMMA particles, PMMA-coated PCM, and graphite particles. In all cases, we could show that the capillary suspensions with polymerizable liquid bridges could be used as precursor to make solid porous materials with customizable features. The solid made from PCM particles had a high porosity, aiding in rapid thermal exchange, and the graphite body was conductive. Possible other applications for this processing route are manifold; both polymeric filter media with defined porosity and chemical properties as well as bio-polymeric materials for medical applications such as soft matrix in the artificial tissue engineering or pharmaceutical processing of drugs could be two potential application routes. For direct application of this method in creating porous bodies, further research is needed to describe the microstructure and the mechanical properties of the polymeric bridges between the particles in order to adjust the physical properties for tailor-made porous materials. In particular, one must be able to control how well the bridge adheres to the particles.

Acknowledgements The authors would like to thank Jonas Keller and Christoph Pfeifer for fruitful discussions, as well as Carolyn Benner for contributing of physical properties of Micronal PCM materials and Frank Schultz and Stefanie Stadler from Freudenberg Technology Innovation SE for μ-Tomography images. Furthermore, we would like to thank Volker Zibat from LEM for SEM and 3M for providing glass hollow spheres iM16K, as well as BASF SE for providing the Micronal DS particles and Altuglas International for providing the PMMA particles. Additionally, we would like to acknowledge financial support from the European Research Council under the European Union's Seventh Framework Program (FP/2007-2013)/ERC Grant Agreement no. 335380.

Compliance with ethical standards

Conflict of interest The authors declare that they have no competing interests.

References

1. Kumar R, Bhattacharjee B (2003) Porosity, pore size distribution and in-situ strength of concrete Cem Concr Res 33(1):155–164. doi:10.1016/S0008-8846(02)00942-0

2. Babu CHA, Rao MP, Ratna JV (2010) Controlled-porosity osmotic pump tablets-an overview J Pharm Res Health Care 2(1):114–126
3. Tunón Å, Börjesson E, Frenning G, Alderborn G (2003) Drug release from reservoir pellets compacted with some excipients of different physical properties Eur J Pharm Sci 20(4–5):469–479. doi:10.1016/j.ejps.2003.09.009
4. Tunón Å, Gråsjö J, Alderborn G (2003) Effect of intragranular porosity on compression behaviour of and drug release from reservoir pellets Eur J Pharm Sci 19(5):333–344. doi:10.1016/S0928-0987(03)00106-4
5. Ulbricht M (2006) Advanced functional polymer membranes Polymer 47(7):2217–2262. doi:10.1016/j.polymer.2006.01.084
6. Dittmann J, Koos E, Willenbacher N (2013) Ceramic capillary suspensions: novel processing route for macroporous ceramic materials J Am Ceram Soc 96(2):391–397. doi:10.1111/jace.12126
7. Maurath J, Dittmann J, Schultz N, Willenbacher N (2015) Fabrication of highly porous glass filters using capillary suspension processing Sep Purif Technol 149:470–478. doi:10.1016/j.seppur.2015.06.022
8. Lee M, Park JK, Lee HS, Lane O, Moore RB, McGrath JE, Baird DG (2009) Effects of block length and solution-casting conditions on the final morphology and properties of disulfonated poly(arylene ether sulfone) multiblock copolymer films for proton exchange membranes Polymer 50(25):6129–6138. doi:10.1016/j.polymer.2009.10.023
9. Vankelecom IFJ (2002) Polymeric membranes in catalytic reactors Chem Rev 102(10):3779–3810. doi:10.1021/cr0103468
10. Tabatabaei SH, Carreau PJ, Ajji A (2008) Microporous membranes obtained from polypropylene blend films by stretching J Memb Sci 325(2):772–782. doi:10.1016/j.memsci.2008.09.001
11. Lee SY, Park SY, Song HS (2006) Lamellar crystalline structure of hard elastic HDPE films and its influence on microporous membrane formation Polymer 47(10):3540–3547. doi:10.1016/j.polymer.2006.03.070
12. Tabatabaei SH, Carreau PJ, Ajji A (2009) Microporous membranes obtained from PP/HDPE multilayer films by stretching J Memb Sci 345(1–2):148–159. doi:10.1016/j.memsci.2009.08.038
13. Stropnik C, Germic L, Zerjal B (1996) Morphology variety and formation mechanisms of polymeric membranes prepared by wet phase inversion J Appl Polym Sci 61(10):1821–1830. doi:10.1002/(SICI)1097-4628(19960906)61:10<1821::AID-APP24%3C3.0.CO;2-3
14. Wienk IM, Boom RM, Beerlage MAM, Bulte AMW, Smolders CA, Strathmann H (1996) Recent advances in the formation of phase inversion membranes made from amorphous or semi-crystalline polymers J Memb Sci 113(2):361–371. doi:10.1016/0376-7388(95)00256-1
15. Pinnau I, Freeman BD (1999) Formation and modification of polymeric membranes: overview Membr Form Modif 744:1. doi:10.1021/bk-2000-0744.ch001
16. Li D, Chung TS, Wang R (2004) Morphological aspects and structure control of dual-layer asymmetric hollow fiber membranes formed by a simultaneous co-extrusion approach J Memb Sci 243(1–2):155–175. doi:10.1016/j.memsci.2004.06.014
17. Jeong BH, Hoek VEM, Yan Y, Subramani A, Huang X, Hurwitz G, Ghosh AK, Jawor A (2007) Interfacial polymerization of thin film nanocomposites: a new concept for reverse osmosis membranes J Memb Sci 294(1–2):1–7. doi:10.1016/j.memsci.2007.02.025
18. Song Y, Sun P, Henry LL, Sun B (2005) Mechanisms of structure and performance controlled thin film composite membrane formation via interfacial polymerization process J Memb Sci 251(1–2):67–79. doi:10.1016/j.memsci.2004.10.042
19. Freger V (2003) Nanoscale heterogeneity of polyamide membranes formed by interfacial polymerization Langmuir 19(11):4791–4797. doi:10.1021/la020920q
20. Zou L, Vidalis I, Steele D, Michelmore A, Low SP, Verberk JQJC (2011) Surface hydrophilic modification of RO membranes by plasma polymerization for low organic fouling J Memb Sci 369(1–2):420–428. doi:10.1016/j.memsci.2010.12.023
21. Silverstein MS (2014) Emulsion-templated porous polymers: a retrospective perspective Polym 55(1):304–320. doi:10.1016/j.polymer.2013.08.068
22. Dittmann J, Maurath J, Bitsch B, Willenbacher N (2015) Highly porous materials with unique mechanical properties from smart capillary suspensions Adv Mater 28(8):1689–1696. doi:10.1002/adma.201504910
23. Studart AR, Gonzenbach UT, Akartuna I, Tervoort E, Gauckler LJ (2007) Materials from foams and emulsions stabilized by colloidal particles J Mater Chem 17(31):3283. doi:10.1039/B703255B
24. Yan F, Goedel WA (2004) A simple and effective method for the preparation of porous membranes with three-dimensionally arranged pores Adv Mater 16(11):911–915. doi:10.1002/adma.200306419
25. Hemmerle A, Schröter M, Goehring L (2016) A tunable cohesive granular material Nat Publ Gr:1–12. doi:10.1038/srep35650
26. Kiesow I, Marczewski D, Reinhardt L, Mühlmann M, Possiwan M, Goedel WA (2013) Bicontinuous zeolite polymer composite membranes prepared via float casting J Am Chem Soc 135(11):4380–4388. doi:10.1021/ja311785f
27. Koos E, Willenbacher N (2011) Capillary forces in suspension rheology Science 331(1994):897–900. doi:10.1126/science.1199243
28. Bossler F, Koos E (2016) Structure of particle networks in capillary suspensions with wetting and nonwetting fluids Langmuir 32(6):1489–1501. doi:10.1021/acs.langmuir.5b04246
29. Bossler F, Weyrauch L, Schmidt R, Koos E (2017) Influence of mixing conditions on the rheological properties and structure of capillary suspensions Colloids and Surfaces A: Physicochem Eng Aspects:1–40. doi:10.1016/j.colsurfa.2017.01.026
30. Domenech T, Yang J, Heidlebaugh S, Velankar SS (2016) Three distinct open-pore morphologies from a single particle-filled polymer blend Phys Chem Chem Phys 18(6):4310–4315. doi:10.1039/C5CP07576A
31. Uemura T, Kitagawa S (2006) Polymerization in confined geometries. In: Materials Science and Technology, Wiley-VCH Verlag GmbH & Co. KGaA
32. Petrie RJ (2006) Polymerization in confined geometries. North Carolina State University, Dissertation
33. de Rooij R, Potanin AA, van den Ende D, Mellema J (1993) steady shear viscosity of weakly aggregating polystyrene latex dispersions J Chem Phys 99(11):9213. doi:10.1063/1.465537
34. Zhang J, Zhao H, Li W, Xu M, Liu H (2015) Multiple effects of the second fluid on suspension viscosity Sci Rep 5(130):16058. doi:10.1038/srep16058
35. Domenech T, Velankar S (2014) Capillary-driven percolating networks in ternary blends of immiscible polymers and silica particles Rheol Acta 53(8):593–605. doi:10.1007/s00397-014-0776-0
36. Velankar SS (2015) A non-equilibrium state diagram for liquid/fluid/particle mixtures Soft Matter 11:8393–8403. doi:10.1039/C5SM01901J
37. Bovey FA, Jelinski L, Mirau PA (1988) Nuclear magnetic resonance spectroscopy. ACADEMIC PRESS, San Diego
38. Smith LM, Coote ML (2013) Effect of temperature and solvent on polymer tacticity in the free-radical polymerization of styrene and methyl methacrylate J Polym Sci Part A Polym Chem 51(16):3351–3358. doi:10.1002/pola.26745
39. Matyjaszewski K (2010) Radical polymerization. Wiley, Encyclopedia of Polymer Science and Technology, pp. 359–473
40. Odian G (2004) Principles of polymerization. Wiley, New Jersey
41. Moad G (2012) Radical polymerization. Elsevier, Clayton, pp. 59–118

42. Ober CK, Lok KP (1987) Formation of large monodisperse copolymer particles by dispersion polymerization Macromolecules 20(2):268–273. doi:10.1021/ma00168a007
43. Paine AJ, Luymes W, McNulty J (1990) Dispersion polymerization of styrene in polar solvents. 6. Influence of reaction parameters on particle size and molecular weight in poly(N-vinylpyrrolidone)-stabilized reactions Macromolecules 23(12):3104–3109. doi:10.1021/ma00214a012
44. Gibson LJ, Ashby MF (1997) Cellular solids: structure and properties. Cambridge University Press, Cambridge